Effect of Polymerization Method on Structure and Properties of Cationic Polyacrylamide

Yinghua Shen, Aiqin Zhang, Genzhuang Wu

College of Chemistry and Chemical Engineering, Taiyuan University of Technology, Taiyuan 030024, People's Republic of China

Received 21 August 2007; accepted 17 June 2008
DOI 10.1002/app.28941
Published online 19 September 2008 in Wiley InterScience (www.interscience.wiley.com).

ABSTRACT: Acrylamide and 2-(methacryloyloxy)ethyltrimethylammonium chloride (AM/MADQUAT) copolymers were synthesized by solution and inverse microemulsion polymerization using $(NH_4)_2S_2O_8/NaHSO_3$ as redox initiator at the same feed mole ratio, and their microstructure, such as sequence distribution and composition distribution, was calculated from monomer reactivity ratios of different polymerization methods. The results show that charge distribution is more uniform for copolymer prepared in inverse microemulsion than that in solution, and copolymer composition distribution is close to unity, and maintains approximately at the feed ratio. Furthermore, the influence of the two structures of cationic polyacrylamides on kaolinite floc size and effective floc density, reduction of Zeta potential and floc compressive yield stress had been investigated at pH 7. The results show that the kaolinite floc size and effective floc density are strongly dependent upon copolymer microstructure, with greater floc size and lower effective floc density being observed for copolymer prepared in inverse microemulsion than for that in solution. Copolymer microstructure has a marked effect on the Zeta potential, whose reduction in the magnitude was much greater in the presence of copolymer prepared in inverse microemulsion than that in solution. Greater compressive yield stress was achieved for the strong flocs produced by copolymer prepared in inverse microemulsion than for the weak flocs produced by that in solution. The difference in flocs compressive yield stress may be attributed to flocs structure. Therefore, in this article, a correlation between the cationic polyacrylamide structure and flocculation property for kaolinite suspension was established. © 2008 Wiley Periodicals, Inc. J Appl Polym Sci 110: 3889–3896, 2008

Key words: water-soluble polymer; copolymerization; microstructure; kaolinite flocculation; structure-property relation

INTRODUCTION

Composition distribution and sequence distribution occupy an important place in microstructure of copolymer. They depend on monomer reactivity ratios, which in turn depend on parameters such as temperature, pH value, as well as added salts. Besides, monomer reactivity ratios are influenced by polymerization method. Candau et al.[1,2] carried out comparison study about monomer reactivity ratios and microstructure of copolymer prepared in solution and inverse microemulsion. They disclosed that the reactivity ratios in inverse microemulsion polymerization were close to unity, and the copolymer prepared in inverse microemulsion had more homogeneous in composition than that in solution.

Correspondence to: Y. Shen (shenyinghua@tyut.edu.cn).

Contract grant sponsor: The Natural Science Foundation of Shanxi Province; contract grant number: 20031018.

Contract grant sponsor: Key Technologies Program of Shanxi Province; contract grant number: 2006031139.

Acrylamide-based cationic polymers are widely used in a variety of industrial applications in the treatment of sewage, the clarification of industrial wastewater, solids/liquid separation, and in papermaking as strength additives, flocculation[3], drainage and retention aids, corrosion inhibition[4] etc. Acrylamide(AM) and 2-(methacryloyloxy)ethyltrimethylammonium chloride (MADQUAT) copolymers (p(AM-MADQUAT)) is one of cationic acrylamide-based polymers containing quaternary amine group, and it is synthesized by solution polymerization conventionally, wherein resultant polymer has a less uniform monomer distribution. Because the monomer unit distribution in the polymer is created by the reactivity ratios of the monomer involved, polymerization must employ monomers having relatively similar reactivity ratios to get the uniform distribution polymers. While in recent years, Candau et al.[1] showed that monomer reactivity ratios in inverse microemulsion polymerization were close to similarity. As for monomer reactivity ratios of AM and MADQUAT, they were reported in solution polymerization[5] and inverse microemulsion polymerization method,[6] respectively. But few, if any, reports

can be found about monomer reactivity ratios of AM and MADQUAT in solution and inverse microemulsion polymerization at the same polymerization conditions, and much less attention was paid to the effect of cationic polyacrylamide microstructure on properties.

In present article, in an attempt to gain some further information regarding effect of microstructure of p (AM-MADQUAT) on flocculant properties, we performed initial investigation: Copolymer composition was simulated by terminal model at high conversion. The sequence distribution of copolymer was calculated from reactivity ratios. To compare with flocculant efficiency of p(AM-MADQUAT) prepared in solution and inverse microemulsion, floc size, effective floc density, compressive yield stress, and reduction of Zeta potential had been studied for kaolinite suspension at pH 7.

THEORY

Floc size

The Richardson and Zaki[7] equation for the group-settling rate for uniform spherical particles can be written:

$$Q = V_{SA}\varepsilon^{4.65} \tag{1}$$

where Q is settling rate of slurry-supernatant interface (cm h^{-1}), V_{SA} is Stokes' velocity for single floc (cm h^{-1}), ε is void fraction.

Michaels and Bolger[8] suggest that the floc diameter, d_A, is relatively independent of kaolinite concentration over the "dilute" range, and that d_A doesn't change once settling has begun. The dilute settling rate should then be given by eq. (1) in the form:

$$Q_0 = \frac{g(\rho_A - \rho_w){d_A}^2}{18\mu_W}(1 - \phi_A)^{4.65} \tag{2}$$

where, Q_0 is initial settling rate of slurry-supernatant interface (cm h^{-1}), d_A is average floc diameter (μm), ϕ_A is floc volume fraction, ρ_A is density of flocs (g cm^{-3}), ρ_w is density of water (g cm^{-3}), μ_w is viscosity of water(0.893 cp at 25°C), g is local gravitational acceleration (980 cm s^{-2}).

From a material balance on the kaolinite, Nasser and James[9] report that eq. (2) can be written as the following form:

$$Q_0 = \frac{g(\rho_K - \rho_W){d_A}^2}{18\mu_W C_{AK}}(1 - C_{AK}\phi_K)^{4.65} \tag{3}$$

where, $C_{AK} = \frac{\phi_A}{\phi_K}$, ϕ_k is kaolinite volume fraction, ρ_k is density of kaolinite (2.6 g cm^{-3}).

$$\text{Due to } V_{SA} = \frac{g(\rho_k - \rho_w){d_A}^2}{18\mu_w C_{AK}} \tag{4}$$

Equation (3) can be rewritten as[7]:

$${Q_0}^{1/4.65} = {V_{SA}}^{1/4.65}(1 - C_{AK}\phi_K) \tag{5}$$

If one plots ${Q_0}^{1/4.65}$ against the corresponding value of ϕ_k, a tendency line should result. From the values of the slope and intercept one, can estimate the floc size.

Effective floc density

It is believed that the floc density is a crucial factor in determining the efficiency of the solid-liquid separation process. According to results of Tambo and Watanabe,[10] they suggest that the floc density can be estimated using a modified Stokes' Equation. Stokes' setting equation for discrete particles is:

$$V_{SA} = \sqrt{\frac{4g\rho_e d_A}{3C_D\rho_w}} \tag{6}$$

where, V_{SA} is Stokes' velocity for single floc (cm s^{-1}), d_A is the floc diameter (cm), ρ_e the effective floc density (g cm^{-3}), C_D is the drag coefficient which is a function of the particle Reynolds number (Re) and sphericity. Tambo and Watanabe[10] observe that when Reynolds number is less than 10^6 implies that the flocs settle is in the laminar region where $C_D = 45/Re$. Thus the effective floc density can be calculated from using eq. (7).[11]

$$\rho_e = \frac{135\mu_w V_{SA}}{4g{d_A}^2} \tag{7}$$

Compressive yield stress

Buscall and White[12] estimated the compressive yield stress [$p_y(\phi)$] of latex and bentonite suspensions from batch centrifuge experiments. The experiments utilized a centrifuge to consolidate to equilibrium sediments of material at each of a series of consecutively increasing gravitational fields. It was concluded that, for most practical applications, the use of a mean value approximation for the determination of $p_y(\phi)$ from equilibrium sediment height data was sufficiently accurate. The mean value approximation allows determination of $p_y(\phi)$[12]:

$$p_y(\phi) = \Delta\rho a\phi_0 h_0\left(1 - \frac{h_\infty}{2R}\right) \tag{8}$$

TABLE I
Copolymer and Correlated Parameters

Copolymer	Polymerization system	Conversion (%)	Cationic degree/mol %	Intrinsic viscosity (mL g^{-1})
S-C8020[a]	Solution	99	19	486
M-C8020[a]	Inverse microemulsion	100	18	536

[a] Feed mole ratio of AM to MADQUAT in C8020 is 80 : 20

$$\phi = \frac{\phi_0 h_0 \left[1 - \left(\frac{h_\infty + s}{2R}\right)\right]}{\left[(h_\infty + s)\left(1 - \frac{h_\infty}{R}\right) + \frac{h_\infty{}^2}{2R}\right]} \quad (9)$$

where, $\Delta\rho$ is the density D-value of solid to liquid (g cm^{-3}), a is the centrifugal acceleration ($\alpha = \omega^2 R$) (m s^{-2}), ϕ_0 is initial volume fraction of solids, h_0 is initial height of the suspension (m), h_∞ is the equilibrium height (m), R the radius of rotation at the bottom of the sediment (m), s is the slope and $s = \frac{dh_\infty}{d \ln a}$, and ϕ is volume fraction of solids.

Plotting the compressive yield stress $p_y(\phi)$ as function of solid volume fraction ϕ, a relationship curve should result.

EXPERIMENAL

Materials

Acrylamide (AM), which is AR, was supplied by Jiangxi Agriculture and Science Chemical Industry (Jiuchang,China). 2-(methacryloyloxy)ethyltrimethylammonium chloride (MADQUAT) was supplied by Xinyu Chemical Industry (Wuxi, China)as a 76.33% wt/wt aqueous solution and used as received. Ammonium persulfate($(NH_4)_2S_2O_8$), sodium hydrosulfite ($NaHSO_3$), cyclohexane and acetone were AR grade reagents and used as supplied. Potassium polyvinyl sulfate (PVSK) and toluidine blue were obtained from Wako Pure Chemical Industries, Osaka, Japan. Kaolinite was supplied by Yicheng Clay Mill (Shanxi, China),and grain size is 200 meshes. Deionized water was used in the present experiment.

Polymerization procedure

Solution polymerization

The polymerization experiments were carried out in water-jacketed reaction vessels, the total concentration of two monomers was kept constant at 1.5 mol L^{-1} (pH 6.5). The solution was bubbled with purified nitrogen to remove oxygen, then was initiated with redox initiator [m $(NH_4)_2S_2O_8$) : m ($NaHSO_3$) = 2 : 1] at 30°C.The initiator concentration was constant (0.04 mol L^{-1} based on solution). After polymerization for 6 h, latices were poured into an excess of acetone and the precipitated copolymers were separated and washed several times. They were then dried under vacuum at 40°C for 6 h. Conversion was determined gravimetrically.

Inverse microemulsion polymerization

The transparent and thermodynamically stable microemulsion was prepared by stirring and adding the aqueous solution of monomers (pH 6.5) to mixture emulsifiers of Span20 and Tween80.The recipe used was the following (wt/wt): monomer aqueous solution 30%, cyclohexane 60% and mixture emulsifiers 10%. After bubbling purified nitrogen through the microemulsion to eliminate oxygen, the monomers were initiated with redox initiator at 30°C and polymerization completed after 3 h. The other steps were the same as solution polymerization.

Copolymer characteristics

The cationic degree was determined by colloidal titration method[13]. The intrinsic viscosity of polymers was measured by Ubbelohde viscometer(inner diameter of capillary is 0.5 mm) in 1*M* NaCl aqueous solution and at 30°C. Corresponding parameters were listed in Table I.

The sequence distribution of copolymer was calculated from monomer reactivity ratios (in solution, $r_1 = 0.30$, $r_2 = 1.31$; in inverse microemulsion, $r_1 = 0.63$, $r_2 = 1.13$, where subscript 1, 2 represent AM, MADQUAT respectively)[14], which were measured at low conversion (<10%). The composition of copolymer was simulated by computer program using a terminal model at high conversion given by Harwood.[15]

Floc size and effective floc density measurements

Kaolinite suspensions of different volume fraction were prepared in 100 mL cylinder with plug. At optimum dosage, flocculant solution (0.1% wt/wt) was added to kaolinite suspensions at pH 7. After

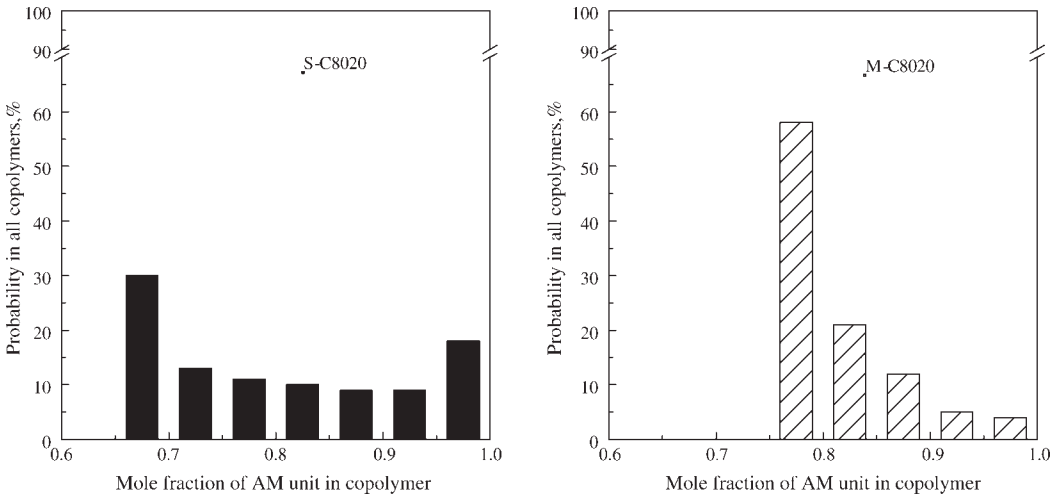

Figure 1 Composition distribution of copolymers with feed mole composition 80 : 20 (AM : MADQUAT).

inverting cylinder 10 times and making the flocculant and kaolinite suspensions mix full, the settling rate was recorded as a function of time. Floc size and effective floc density was estimated according to the method given by Nasser and James.[9]

Zeta potential measurement

At optimum dosage, flocculant solution (0.1% wt/wt) was added to kaolinite suspension (volume fraction 0.02) at pH 7. The kaolinite suspension was agitated by a rotating shaker at 120 rpm for 1 h; the samples were allowed to settle for 20 min to allow the larger particles to settle. An aliquot taken from the supernatant was used to measure the Zeta potential by micro-electrophoresis apparatus trophresis (JS94G+).

Compressive yield stress measurement

A batch centrifuge (Mistral 1000, UK) was used in the compressive yield stress measurements. The centrifuge tubes used in these measurements held 10 mL of suspension and had a diameter of 15 mm. Different rotational speeds in the range of 800–1000 rpm were used. In these measurements, the optimum dosage were used to study the consolidations rate for kaolinite suspensions. Compressive yield stress was measured following the procedure given by Nasser and James.[9]

RESULTS AND DISCUSSION

Composition distribution

Composition distribution of the copolymers with feed mole ratio 80 : 20(AM to MADQUAT) was

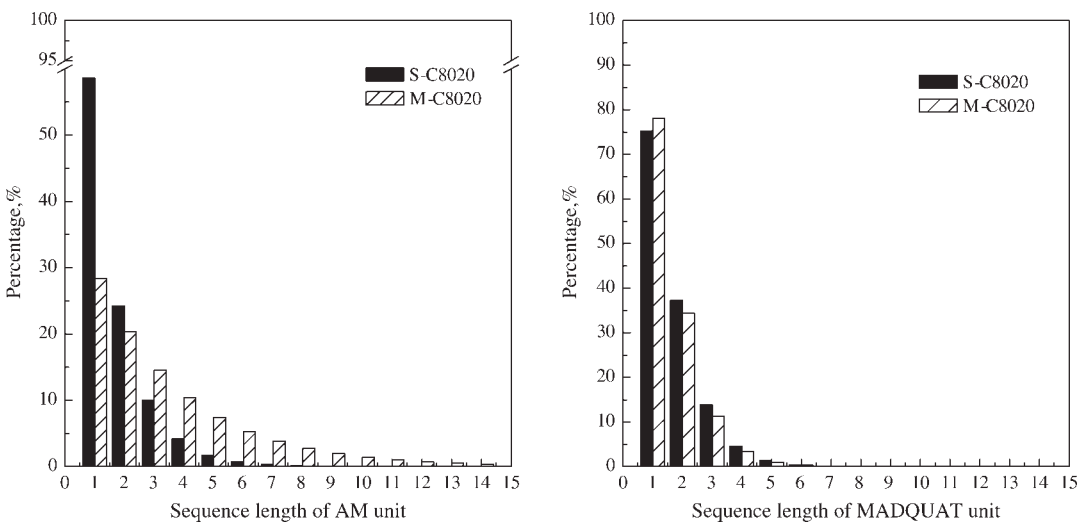

Figure 2 Sequence length distribution of AM and MADQUAT unit in copolymer polymer chain.

TABLE II
Number Average Sequence Length and Run Number

Copolymer	$\bar{l}_1$	$\bar{l}_2$	R (100 monomer unit)
S-C8020	2.20	1.33	56.70
M-C8020	3.52	1.28	41.64

simulated by computer program according to terminal model at high conversion, as shown in Figure 1. It can be seen that composition distribution of *S*-C8020 appeared to be U-shaped, while composition distribution of M-C8020 appeared to be L-shaped. The composition distribution of M-C8020 was closer to feed ratio than that of *S*-C8020. The results suggest that the composition distribution of M-C8020 was more uniform than that of *S*-C8020.

Sequence length distribution

Sequence length distribution of obtained copolymers was calculated from reactivity ratios, as shown in Figure 2. It can be seen that the probability of 3 AM. and those of more than 3 AM. sequences in M-C8020 was higher than that in *S*-C8020, and the probability of 1MADQUAT sequence was the highest among the MADQUAT sequences in both M-C8020 and *S*-C8020. Therefore, the probability of alternation of 3 AM. and those of more than 3 AM. sequences or with 1MADQUAT sequence was high in M-C8020. Although the probability of alternation of 1 AM. or 2 AM. sequences with 1MADQUAT sequence was high in *S*-C8020. As a result, cationic group distribution in M-C8020 was more uniform than that in *S*-C8020. In other words, sequence distribution of copolymer prepared in inverse microemulsion is more homogeneous than that in solution.

Number average sequence length and run number

According to first-order Markov model, number average sequence length $\bar{l}_1$ and $\bar{l}_2$, which are monomer units in per monomer segment, for AM and MADQUAT in the copolymer were calculated according to the method of Pynn[16] utilizing eqs. (10) and (11), respectively.

$$\bar{l}_1 = 1 + r_1 x \tag{10}$$

$$\bar{l}_2 = 1 + r_2/x \tag{11}$$

where, x is the monomer feed mole fraction of AM to MADQUAT.

The run number R of copolymer is defined as the average number of sequence of either types per 100 monomer units, which gives the population of monomer units in the copolymer.[17] Run number R was calculated using the sequence length of $\bar{l}_1$, $\bar{l}_2$ as eq. (12)

$$R = \frac{200}{\bar{l}_1 + \bar{l}_2} \tag{12}$$

The calculated results were given in Table II. From the results in Table II, according to run number R in either types per 20 monomer units and number average sequence length, their polymer chain models were predicted as shown in Figure 3.

The earlier model reflected charge distribution in the polymer chain at polymerization primary stage. With increase of conversion, cationic monomer in solution polymerization was consumed rapidly, and led to few cationic groups in polymer chain at polymerization final stage; while in inverse microemulsion polymerization, due to uniform monomer reactivity ratios, the content of cationic monomer maintained approximately at the initial feed fraction, so the charge distribution in polymer chain changed hardly throughout polymerization. This conclusion is consistent with earlier sequence distribution and in good concordance with the collision mechanism given by Candau et al.,[18] who described that in inverse microemulsion, polymer chain propagated chiefly by collision between nucleated and unnucleated particles, and the monomer proportions at the reaction sites should be maintained at their initial values throughout the polymerization, thus generating a homogeneous microstructure.

Floc size and effective floc density

According to eq. (5), plots $Q_0^{1/4.65}$ against the corresponding value of ϕ_k, a tendency line should result, the obtained tendency lines for M-C8020 and *S*-C8020 were shown in Figure 4, and the values of

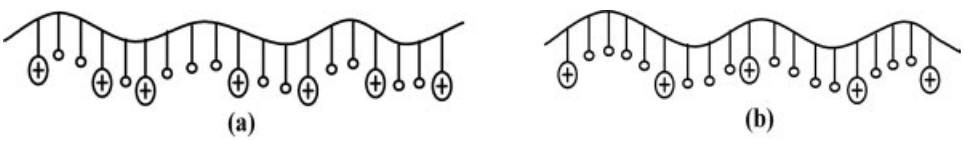

Figure 3 Polymer chain model of copolymer prepared by different polymerization method at low conversion: (a) *S*-C8020; (b) M-C8020 (○ AM monomer unit ⊕ MADQUAT monomer unit).

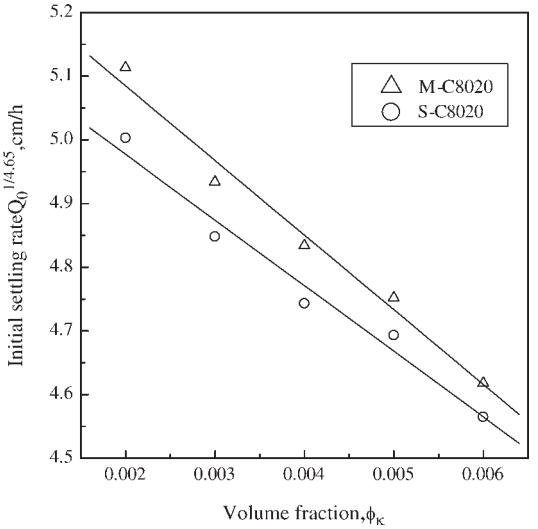

Figure 4 Initial settling rates as a function of volume fraction.

slope and intercept were listed in Table III. From the values of the slope and intercept one, the values of the floc size and effective floc density calculated utilizing eq. (4) and (7) for M-C8020 and *S*-C8020 were shown in Table III. The results show that the floc size of the kaolinite produced by M-C8020 was larger than that for *S*-C8020, and the effective floc density was lower for M-C8020 than that for *S*-C8020.

This observation can be supported by the different composition distribution of M-C8020 and *S*-C8020 : composition distribution of M-C8020 was more uniform than that of *S*-C8020. Furthermore, it can be also obtained from Figure 1 that copolymer which AM mole fraction was 0.675 and 0.725 made up 43% of all copolymer in *S*-C8020, while copolymer which AM mole fraction was 0.775 and 0.825 made up 79% of all copolymer in M-C8020. Because of the steric effect, the content of MADQUAT unit is higher, the length of the polymer chain is short, and the molecular weight is low. It is possible that polymer of low molecular weight in *S*-C8020 make up higher fraction than that in M-C8020, and the bridging ability of flocculation of *S*-C8020 should be weak than that of M-C8020. So kaolinite suspension treated by *S*-C8020 could produce plenty of little flocs, which decreased flocculation efficiency of *S*-C8020. Therefore, strong bridging ability allows M-C8020 to produce greater floc size than that for *S*-C8020. However, greater floc size cause the larger interfloc porosity, which leads to the lower effective floc density, so M-C8020 demonstrates lower effective floc density than *S*-C8020.

Zeta potential (ζ)

Figure 5 shows that the ζ image of supernatant of kaolinite suspensions treated by *S*-C8020 and M-C8020 respectively. Magnitudes of Zeta potential before flocculation and after flocculation and the corresponding reduction of Zeta potential were shown in Table IV. The results demonstrated that the reduction of ζ for M-C8020 was greater than that for *S*-C8020. This could be explained by charge distribution of copolymer. Earlier findings show that charge distribution of M-8020 was more uniform than that of *S*-C8020. Because of the MADQUAT unit containing heavy pendant group, when MADQUAT units concentrate, cationic groups are much more influenced by steric effect in flocculation process, and a few cationic groups have no chance to adhere onto kaolinite particles[19]. Therefore, the number of cationic group contacted with the negatively charged Kaolinite particles in *S*-C8020 was less than that in M-C8020, that is to say, effective cationic groups in *S*-C8020 were less than in M-C8020. Consequently, *S*-C8020 showed weaker ability of compressing the electrical double layer and produced lower reduction of Zeta potential than M-C8020.

Compressive yield stress

Figure 6 shows the relationship between compressive yield stress and solid volume fraction for sediments using the two copolymers at optimum dosage. Present results show that the compressive yield stress, $p_y(\phi)$, for M-C8020 was higher than that for *S*-C8020. An explanatory summary of sediment bed behavior of kaolinite treated by the two copolymers is depicted in Figure 7. Starting with similar volume fraction of kaolinite and settling/centrifuging columns, both flocculated suspensions show similar initial suspension heights (h_0) but different floc structures. Strong powerful bridging ability allows M-C8020 to produce greater floc size and interfloc porosity than *S*-C8020 and strong charge neutralization of M-C8020 destabilizes kaolinite suspension, and facilitated flocculation, which lead that M-C8020 produced strong flocs, while *S*-C8020 produced

TABLE III
Floc Structure Parameters Obtained from Settling Rate Data at pH 7

Copolymer	Slope	Intercept	C_{AK}	V_{SA} (cm h^{-1})	d_A (μm)	ρ_e (g cm^{-3})
M-C8020	−117.28	5.3195	22.031	2380	388	0.1353
S-C8020	−103.09	5.1834	19.888	2103	346	0.1499

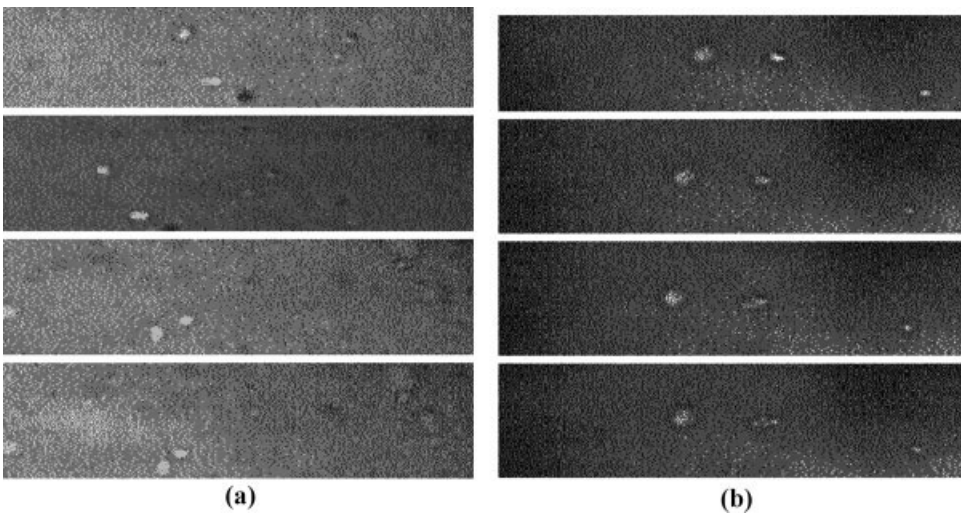

Figure 5 Zeta potential image of kaolinite supernatant treated by polymer: (a) *S*-C8020; (b) M-C8020

weak and fragile flocs. Under compressive load, the strong flocs produced by M-C8020 are capable of resisting deformation; thereby producing a less compact sediments that corresponds to a high compressive yield stress. This was apparent from the obtained equilibrium sediment heights (h_∞) found following centrifugation. The flocs produced by *S*-C8020 tended to be open and more deformable, and thereby produced more compact sediments and a low compressive yield stress.

CONCLUSIONS

The influence of copolymer of composition distribution and sequence distribution on floc size, effective floc density, the reduction of Zeta potential, and compressive yield stress in the flocculation-sedimentation process for negatively charged kaolinite suspensions was investigated to compare flocculation properties of the two copolymers prepared in inverse microemulsion and in solution. The following conclusions have been drawn:

Compared with the copolymer prepared in solution, the copolymer prepared in inverse microemulsion shows uniform sequence distribution and composition distribution, in good agreement with the results by Candau et al.

TABLE IV
Magnitude of Zeta Potential and Reduction of Zeta Potential

Copolymer	ζ_0 (mV)	ζ_1 (mV)	$\Delta\zeta$ (mV)
M-C8020	−27.236	−2.0254	25.2106
S-C8020	−27.236	−7.2859	19.9501

ζ_0: before flocculation; ζ_1: after flocculation; $\Delta\zeta = \zeta_1 - \zeta_0$.

The floc size and effective floc density depend on copolymer microstucture strongly. Larger floc size and lower effective floc density were achieved using copolymer prepared in inverse microemulsion than using that in solution.

Copolymer microstructure has a marked effect on the Zeta potential, whose reduction in the magnitude was much greater in the presence of copolymer prepared in inverse microemulsion than that in solution.

The magnitude of the compressive yield stress is strongly dependent upon the floc structure, with greater compressive yield stress being observed for the strong flocs produced by copolymer prepared in inverse microemulsion than for the weak flocs produced by that in solution.

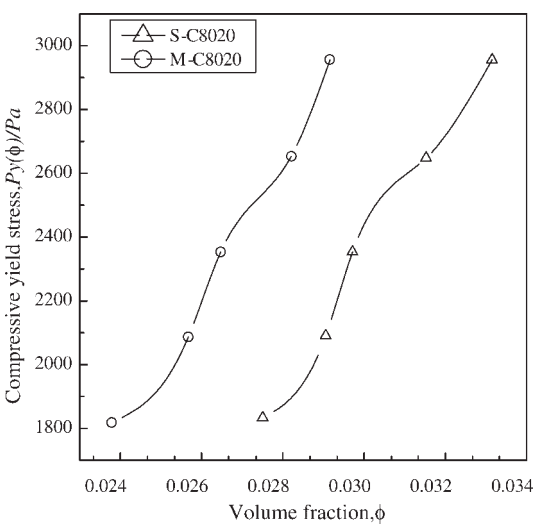

Figure 6 Compressive yield stresses $p_y(\phi)$ as functions of solid volume fraction ϕ.

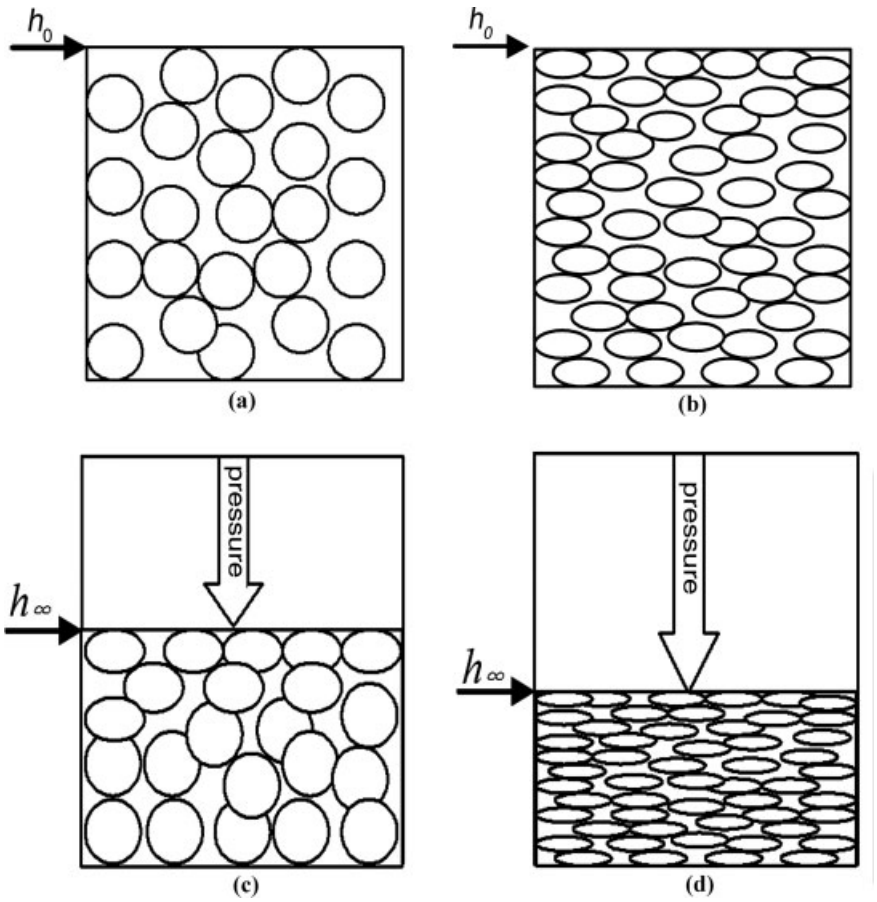

Figure 7 Schematic diagram showing ways in which different flocs structure produces different equilibrium sediment height. 1. Starting with similar initial volume fraction of kaolinite and suspension height (above the (a) (b) figures). (a) M-C8020 (b) S-C8020. 2. Sediment bed behavior after centrifugations in a similar compression load (above the (c) (d) figures). (c) High compressive yield stress (d) Low compressive yield stress.

References

1. Candau, F.; Zekhnini, Z.; Heately, F.; Franta, E. Colloid Polym Sci 1986, 264, 676.
2. Corpart, J. M.; Selb, J.; Candau, F. Polymer 1993, 34, 3873.
3. Escudero Sanz, F. J.; Ochoa Go'mez, J. R.; Sasia, P. M.; Gi'az de Apodaca, E.; Ri'o, P. J Appl Polym Sci 2007, 103, 2826.
4. Gao, B. J.; Lv, Y. X.; Jiu, H. F. Polym Int 2003, 52, 1468.
5. Tanaka, H. J Polym Sci Polym Chem Ed 1986, 24, 29.
6. Kozakiewicz, J. J.; Lipp, D. W. U.S. Pat. 285938 (1988).
7. Richardson, J. F.; Zaki, W. N. Trans Inst Chem Eng 1954, 32, 35.
8. Michaels, A. S.; Bolger, J. C. Ind Eng Chem Fund 1962, 1, 24.
9. Nasser, M. S.; James, A. E. Sep Purif Technol 2006, 52, 241.
10. Tambo, N.; Watanabe, Y. Water Res 1979, 11, 409.
11. Nasser, M. S.; James, A. E. Colloids Surf A: Physicochem Eng Aspects 2007, 301, 311.
12. Buscall, R.; White, L. R. Adv Colloidal Interface Sci 1994, 51, 175.
13. Terayama, H. J Polym Sci 1952, 8, 243.
14. Shen, Y. H.; Wu, G. Z.; Wang, S. X. Polym Mater Sic Eng (China) 2008, 24, 23.
15. Harwood, H. J J Polym Sci C 1968, 25, 37.
16. Pynn, C. W. J Polym Sci 1990, A2, 1111.
17. Harwood, H. J.; Ritchey, W. M. Polym Lett 1964, 2, 601.
18. Candau, F.; Leong, Y. S.; Fitch, R. M. J Polym Sci Polym Chem Edn 1985, 23, 193.
19. Mpofu, P.; Addai-Mensah, J.; Ralston, J. Miner Eng 2004, 17, 411.